

## Solution Self-Assembly of Magnetic Light Modulators from Exfoliated Perovskite and Magnetite Nanoparticles

Frank E. Osterloh\*

Department of Chemistry, University of California at Davis, Davis, California 95616

Received February 7, 2002

As intermediates between the molecular and the solid states, inorganic nanoparticles<sup>1,2</sup> combine chemical accessibility in solution with physical properties of the bulk phase. They are thus ideal elements for the construction of nanostructured materials and devices with adjustable physical and chemical properties. As an example for this building principle, we present here the synthesis of nanostructured particle aggregates by covalent linkage of soluble  $(\text{Bu}_4\text{N})_x[\text{H}_{1-x}\text{Ca}_2\text{Nb}_3\text{O}_{10}]$  nanosheets<sup>3</sup> (from a layered perovskite) and superparamagnetic  $\text{Fe}_3\text{O}_4$  spheres.<sup>4</sup> Due to optical anisotropy of the sheets and the superparamagnetism of the magnetite particles, the nanoparticle aggregates exhibit magnetically controllable birefringence and light-scattering properties in solution, which make the composite interesting for magneto-optical sensing, display, and data storage applications.

The title compound was synthesized by combining solutions of oleic acid-ligated magnetite particles and of 3-aminopropylsilylated  $[\text{H}_{1-x}\text{Ca}_2\text{Nb}_3\text{O}_{10}]^{x-}$  colloidal sheets in tetrahydrofuran.<sup>5</sup> When ethanol is added to the resultant mixture, the magnetite particles precipitate onto the perovskite sheets, and the product forms. After centrifugation and washing with THF, the composite is obtained as a brown-beige solid, which can be easily dispersed in ethanol, hexane, or THF to give beige to brown suspensions, depending on concentration.

Scanning electron and scanning probe micrographs reveal that the composite particles consist of stacks of 2-nm thick  $(\text{Bu}_4\text{N})_x\text{-}[\{\text{NH}_2(\text{CH}_2)_3\text{Si}\}_n\text{H}_{1-x}\text{Ca}_2\text{Nb}_3\text{O}_{10}]$  sheets ( $300 \times 300$  nm), which are covered 9-nm magnetite particles, most of which are aggregated into clusters of 2–30 particles. Stacks are 50–110 nm high and have average lateral dimensions of  $8 \times 8 \mu\text{m}$  (Figure 1a). A typical stack contains about 15 000 perovskite sheets and about 14 000 magnetite particles. Smaller stacks (Figure 1b;  $1.0 \times 1.0 \times 0.03\text{--}0.09 \mu\text{m}$ ) form when the functionalization of  $[\text{H}_{1-x}\text{Ca}_2\text{Nb}_3\text{O}_{10}]^{x-}$  with 3-aminopropyltrimethoxysilane is performed in ethanol, where the solubility of colloidal sheets is higher and the aggregation tendency is reduced. A typical composite particle of this group contains about 400 perovskite sheets (individual sheets are visible in Figure 1b) and 300 magnetite particles. Because non-aminated perovskite sheets also exhibit a weak affinity to oleic acid ligated  $\text{Fe}_3\text{O}_4$  particles, the bonding in the aggregates is believed to involve both van der Waals and covalent interactions between  $\text{NH}_2$  groups and  $\text{Fe}_3\text{O}_4$  particles.

Similar to the pure or amine-modified perovskite starting materials, dilute dispersions of the composite are opalescent due to light reflection, scattering, and absorption by randomly oriented nano- and microparticles. In a magnetic field ( $H > 10$  G), the anisotropic aggregates adopt a preferential orientation, and refractive index and light-scattering properties assume a directional depend-

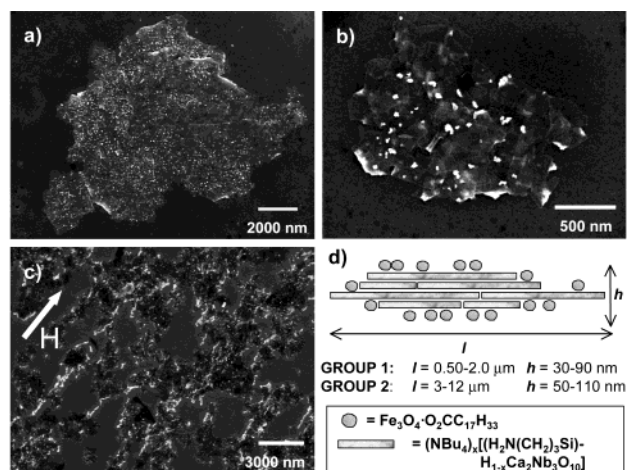


**Figure 1.** Scanning electron micrographs (secondary electrons) of the perovskite–magnetite composite. (a) Large aggregate, (b) Small aggregate, (c) Strings of aggregates formed in a homogeneous field (2 T) in the indicated direction. (d) Schematic structure of magnetite–perovskite aggregates.

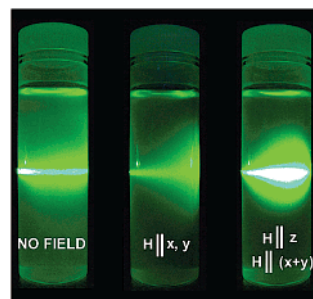


**Figure 2.** Propagation of laser light (500–550 nm) through a dilute suspension of  $(\text{Bu}_4\text{N})_x[\text{H}_{1-x}\text{Ca}_2\text{Nb}_3\text{O}_{10}\text{-NH}_2]\cdot[\text{Fe}_3\text{O}_4\text{-OA}]$  in THF in the absence and presence of magnetic fields (1000 Oe) with the indicated orientations. Axes are labeled as in Figure 3.

ence, that is, the suspension becomes birefringent.<sup>6</sup> These effects are demonstrated in Figures 2 and 3a for suspensions of large aggregates, and in Figure 3b for the small aggregates.

Maximum light reflection in  $x$  direction (for axis labels see Figure 3a) occurs when the field lines are along  $z$  or along  $x + y$ ; minimum reflectance occurs for  $H$  along  $x$  or  $y$ . The observed reflection angles are in agreement with geometrical optics, if one assumes that the sheetlike aggregates are aligned with their planes along the lines of the magnetic field. As the emission spectra in Figure 3a show, the scattering intensity  $I_s$  (reflection is essentially a scattering phenomenon) also strongly depends on the wavelength of the incident light.  $I_s$  is largest for green light (450–550 nm) and, due to absorption, diminishes with shorter wavelengths. For light with

\* To whom correspondence should be addressed. E-mail: osterloh@chem.ucdavis.edu.

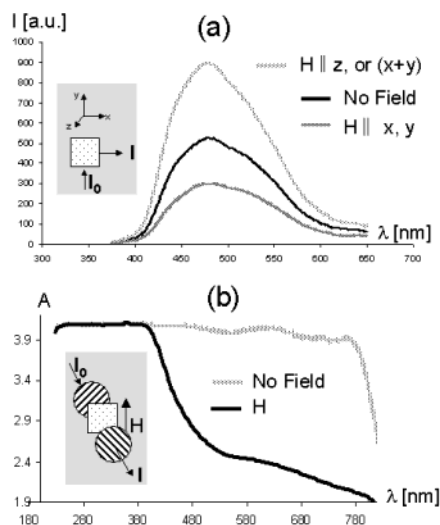


**Figure 3.** (a) Emission spectra of a suspension of the  $>3 \mu\text{m}$  perovskite– $\text{Fe}_3\text{O}_4$  composite in ethanol. The intensities of scattered light are shown for zero and nonzero magnetic fields (1000 Oe) with the indicated orientations. (b) Absorption spectra of a  $<2 \mu\text{m}$  particle suspension placed between two cross-polarized filters. Maximum depolarization is observed under a magnetic field at  $45^\circ$  versus the polarization plane of the incident light.

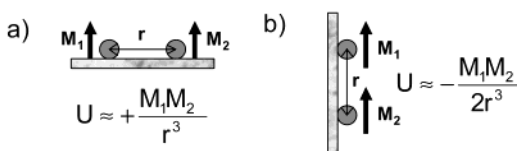


**Figure 4.** Magnetostatic energy of a system of two superparamagnetic particles immobilized on a sheet at distance  $r$  with different orientations of their magnetic moments  $M_{1/2}$  with respect to the plane.

$\lambda > 550 \text{ nm}$ ,  $I_s$  drops off quickly due to  $I_s \approx \lambda^{-4}$  (Rayleigh–Debye law).<sup>7</sup>

Because of their reduced size, the small aggregates ( $<2 \mu\text{m}$ ) reflect light only weakly. However, they efficiently depolarize the incident light, when the magnetic field vector forms a  $45^\circ$  angle with the plane of polarization as shown in Figure 3b. Using a setup with two cross-polarized filters, this property would allow the construction of a magnetic light switch.

The observed magnetic birefringence and scattering phenomena are intimately connected with the magnetic properties of the composite. Preliminary magnetization data collected on the magnetite-perovskite composite with a superconducting quantum interference device (SQUID, Supporting Information) reveal its superparamagnetic nature (compare ref<sup>8</sup>). From field-cooled and zero field-cooled magnetization curves, the blocking temperature  $T_B$  for the composite was found to be 210 K. Below  $T_B$  the composite exhibits hysteresis behavior as expected for a ferrimagnetic  $\text{Fe}_3\text{O}_4$  phase,<sup>9</sup> whereas above  $T_B$ , Langevin-type magnetization behavior<sup>10</sup> typical of paramagnetic matter is observed. Interestingly, the dried 9-nm magnetite nanoparticles have a higher blocking temperature ( $T_B = 280 \text{ K}$ ) than the composite, whereas a magnetite particle solution in mineral oil exhibits a lower  $T_B$  (150 K). This trend of increasing  $T_B$  in the row  $\text{Fe}_3\text{O}_4$  solution, dried  $\text{Fe}_3\text{O}_4\text{--Ca}_2\text{Nb}_3\text{O}_{10}$  composite, and dried  $\text{Fe}_3\text{O}_4$  particles reflects increasing dipolar interactions between increasingly clustered particles.

Tentatively, we identify dipolar interactions between adjacent magnetite particles on the perovskite sheets as cause for the observed orientational phenomena of the aggregates in solution. As Figure 4 shows, the magnetostatic energy  $U$  of a pair of two aligned magnetic dipoles depends on their mutual orientation.<sup>10</sup> It

is at maximum for orientation a, with the magnetization vectors  $M_{1/2}$  normal to the plane, and at minimum for orientation b, with  $M_{1/2}$  parallel to the plane. Because of the lower magnetostatic energy for configuration b, a planar array of  $\text{Fe}_3\text{O}_4$  particles on a perovskite sheet will prefer a collinear alignment of magnetic moments with respect to the plane. The result of this magnetic anisotropy<sup>10</sup> is a preferential magnetization of the sheets along their planes. In an external magnetic field, the sheets then align parallel to the force lines, similar to compass needles.

Dipolar interactions also govern the interactions between individual aggregates. When the stacks are deposited on a surface in a magnetic field, strings of aggregated particles form along the field lines (Figure 1c). Energetically favorable “head-to-tail” arrangements of this kind are typical of superparamagnetic particles.<sup>11,12</sup>

In conclusion we have shown, that superparamagnetic and optically anisotropic colloidal building blocks can be connected using simple chemical strategies to give nanostructured composites with useful magneto-optical properties. A report describing further details of the synthesis of the composite particles and a quantitative analysis of their magnetic characteristics is in preparation.

**Acknowledgment.** Thanks to Professor Kai Liu (UCD, Physics) for magnetization measurements and for review of the manuscript. This work was supported by start-up funds of the University of California at Davis.

**Supporting Information Available:** Scanning electron micrographs of composite particles, magnetization data, AFM profile scans (PDF). This material is available free of charge via the Internet at <http://pubs.acs.org>.

## References

- (1) Murray, C. B.; Kagan, C. R.; Bawendi, M. G. *Annu. Rev. Mater. Sci.* **2000**, *30*, 545–610.
- (2) Aiken, J. D.; Finke, R. G. *J. Mol. Catal. A: Chem.* **1999**, *145*, 1–44.
- (3) Schaak, R. E.; Mallouk, T. E. *Chem. Mater.* **2000**, *12*, 2513–2516.
- (4) Sahoo, Y.; Pizem, H.; Fried, T.; Golodnitsky, D.; Burstein, L.; Sukenik, C. N.; Markovich, G. *Langmuir* **2001**, *17*, 7907–7911.
- (5)  $\text{Fe}_3\text{O}_4\text{--oleic acid}^4$  and  $[\text{Bu}_4\text{N}]_x[\text{H}_{1-x}\text{Ca}_2\text{Nb}_3\text{O}_{10}]$  (9-nm-sized particles)<sup>3</sup> were synthesized as described previously. Ligation with 3-aminopropylsilane was performed in ethanol or tetrahydrofuran (used as received) at room temperature by adding 40 mg of 3-aminopropyltrimethoxysilane to a stirred suspension of 20 mg of  $[\text{Bu}_4\text{N}]_x[\text{H}_{1-x}\text{Ca}_2\text{Nb}_3\text{O}_{10}]$  in 1 mL of the respective solvent. After 1 h, the solid was centrifuged off and washed three times with fresh solvent. Ligation was confirmed with ninhydrin. Ligated particles were suspended in 1 mL of THF, and a solution of 10 mg of oleic acid-ligated  $\text{Fe}_3\text{O}_4$  particles was added in 1 mL of THF. Over 10 min, 3 mL of ethanol was then added to the rapidly stirred mixture to induce product formation. The brown solid was centrifuged off and washed three times with THF to dissolve free  $\text{Fe}_3\text{O}_4$ . For optical measurements (Hewlett-Packard 8450A UV/vis and Perkin-Elmer LS50B luminescence spectrometers), the product was dispersed in ethanol; for magnetic measurements the product was dried in air. Samples for SEM (FEI XL30-SFEG)/AFM (Digital Instruments Nanoscope IIIa) were obtained by drying a drop of the sample suspension on  $1 \times 1 \text{ cm}$  pieces cut from a silicon wafer (100).
- (6) Riande, E.; Saiz, E. *Dipole Moments and Birefringence of Polymers*; Prentice Hall: Englewood Cliffs, NJ, 1992.
- (7) Lyklema, H.; Leeuwen, H. P. v.; Vliet, M. v.; Cazabat, A. M. *Fundamentals of Interface and Colloid Science*; Academic Press: London; San Diego, 1991; Chapter 7.
- (8) Decaro, D.; Ely, T. O.; Mari, A.; Chaudret, B.; Snoeck, E.; Respaud, M.; Broto, J. M.; Fert, A. *Chem. Mater.* **1996**, *8*, 1987–1991.
- (9) Cullity, B. D. *Introduction to Magnetic Materials*; Addison-Wesley: Reading, MA, 1972; pp 181.
- (10) Chikazumi, S. O.; Graham, C. D. *Physics of Ferromagnetism*, 2nd ed.; Clarendon Press: Oxford University Press: Oxford, New York, 1997; p 6 and p 266.
- (11) Pileni, M. P. *Adv. Funct. Mater.* **2001**, *11*, 323–336.
- (12) Puentes, V. F.; Krishnan, K. M.; Alivisatos, A. P. *Science* **2001**, *291*, 2115–2117.

JA025858Y